Analytical study of electromagnetic ion cyclotron wave for ring distribution with AC electric field in Saturn magnetosphere

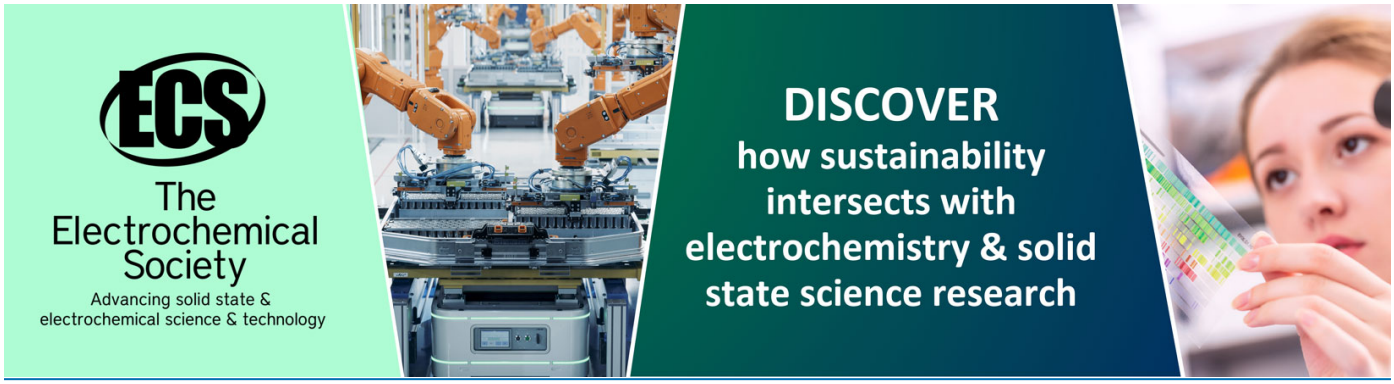

Analytical study of electromagnetic ion cyclotron wave for ring distribution with AC electric field in Saturn magnetosphere

Kumari Neeta Shukla[1], Devi Singh[1] and R.S. Pandey[2]

[1]*Department of Physics, Manav Rachna International Institute of Research and Studies, National Capital Region, Aravali Hills, Sector-43, Faridabad – 121001, Haryana, India;*
[2]*Department of Physics, Amity Institute of Applied Sciences, Amity University, Sector – 125 Noida, Uttar Pradesh, India*

Corresponding author: drdevisingh.fet@mriu.edu.in

Abstract. Characteristics of electromagnetic ion cyclotron waves in Saturn inner magnetosphere has been investigated here in close proximity of equatorial plane at approximately mid of the E ring near 5Rs by using data sets released by Voyager and Cassini spacecraft. Previous encounter of these spacecraft with Saturn exposed the strong signature of EMIC wave and harmonics believed to be originated within 7.5 Rs due to dominant O^+ ions and water group ions. Maxwellian ring distribution for pickup ions contributing ring around planet is opted to find unperturbed particle density. Therefore, investigating here growth of obliquely propagating EMIC wave undergoing wave particle mechanism by opting kinetic approach to establish mathematical dispersion model in view of different parameters and extended to comparative study for parallel propagation. Parametric analysis inferred that waves propagating in the oblique direction grows more as compare to parallel propagating waves for the extended value of temperature anisotropy and the angle of propagation with respect to the ambient magnetic field B (at equator) and second harmonic of ion cyclotron waves indicating that the modified ion cyclotron wave shifts the wave spectra to higher side with increase in bandwidth. Study can be carried out to analyze other instabilities to explore magnetospheric dynamics at different radial distances.

1. Introduction

Saturn is considered to have a huge magnetosphere just after Jupiter in our planetary system orbiting between 9 to 10 AU heliocentric distance. It has unified beautiful ring system with different icy moons placed radially outwards: Mimas, Enceladus, Tethys, Dione, and Rhea revolving around at different radial distances and can be considered as the prominent source of neutral particles. E ring is the widest within all and optically thin extended up to 4 to 5 radiuses i.e. 3Rs to 8Rs (1 Rs = 60,268 km). Constituents of which are micron sized icy watery substance (like O and OH). Inner layer of E ring found denser than outer layer, neutral peak density found near 4 Rs due to venting of molecules of Enceladus lies at 3.8 Rs [1,2].

The outer structure of the E ring is not stagnant. An atomic oxygen cloud appeared in the E ring and gradually decayed in the next two months [3]. This is consistent with the expected short lifetime (less than three months) perhaps due to venting and lost in view of ionization and disintegration of E-ring neutrals [4].

Recent observation by all the spacecraft produced the data which confirms the presence of Ion cyclotron wave associated with observed water group ions within the Saturn E ring. Ion cyclotron wave across the E ring very first detected by Pioneer 11 satellite in the Dione orbital access channel (6.26 Rs) [5], later carried out by Barbosa [6] also confirmed the existence of similar magnetic oscillations coupled to O^+ ion population between 5 - 7 Rs observed by Voyager 1. Likely ion cyclotron waves explored by CAPS magnetometer linked with water group (OH^+, H_2O^+, O^+ and O_2^+) composition again on Cassini's orbit insertion throughout the E ring approximately all the local times with maximum peak close to equator [7,8] gave out the same explanation on these waves during first orbit insertion. Oxygenation was performed almost every time may be due to the continues ionisation process of new born ion. It is evident from the prior studies that low frequency whistler wave or EMIC wave can be generated locally for noticeable redistribution of pitch angle of energetic particles for considerable increases in fluxes and thermal anisotropy. Currently extensive valuation of whistler intensity performed well by [9] below < 10 Rs and achieved maximum intensity of hiss than chorus at high latitude and found it to be constant beyond thirteenth shell (L=13). Guan [10] proposed calculations to analyse linear growth rate of obliquely propagating EMIC wave originated from H+ and He+ in the nightside of radiation belt by using the data provided by Van Allen Probe B.

Harmonic of these ICW with f ~ 2 × WW+ (double the fundamental gyrofrequency of water- group ion) also observed within E ring [7,11] for different length of time scale approximately for 5 hr well evaluated by [12] reporting the presence of ion waves between 4.8 Rs and 5.5 Rs on 24 December and 27 November. Study also confirms the observed harmonics for less time interval (~1h) between 3.8 Rs–4.6 Rs on 9 March fly. During Saturn insertion orbit modified broad band frequency associated with the engine exhaust gas component: CO, N_2, CO_2 and H_2O appeared on the outbound legs of Cassini [13], it is due to ionization of engine exhaust gas component and then acceleration of these generated ions with the co-rotation magnetospheric electric field, thus creating the ring beam distribution in velocity space.

The induced temperature anisotropy basically causes the wave growth by giving free energy to ion cyclotron waves when there occurs significant difference between perpendicular and parallel temperature with respect to magnetic field. Ring beam distribution made up of picked cold neutral ions in the velocity space is the most unstable system in order to magnify waves. These were also detected in Jupiter's and comets magnetosphere explained by [14] and [15] respectively.

Data model produced by [16] reported transportation of energetic charged particle in Saturn magnetospheric layers well explained that inner to middle (8-12 Rs) is adiabatic transport dominant and inner (<7 Rs) is most affected by centrifugally driven injection process associated with interchange instability which is obvious due to interaction with neutral gas torus of E ring, expecting no storage and release of magnetic energies [17,18] due to low particle pressure as compared to magnetic pressure. Inward (hotter) and outward (cooler) radial diffusion are believed to be derived by E ×B drift and gradient-curvature drift. The process is totally energy specific as transported charged particles moves toward stronger magnetic field, consequently acquiring more energy enable the most energetic to penetrate deeper [19]. E rings reason is mainly populated with low mean energy ions moving at coronation velocities and neutral gas Taurus at Keplerian velocities hence lead to wave growth. Seemingly Some of the neutral gas species are ionized due to charge exchange with Saturn magnetospheric plasma charged particle, solar UV radiation and electron collisional impact. Initially new born ions move at the Kepler velocity letter tend to accelerate with Saturn coronation speed (E x B drift along the cycloidal trajectory) on time scale for several days. Consequently, these pickup ions form ring type distribution around planet in velocity phase space and gain higher kinetic energy (in the form of heat) causing ion wave unstable conclusively it was found that the induced Temperature anisotropy between ion profile work as the major source of the growth of EMIC wave [20].

Ion cyclotron wave within the Saturn E ring very first detected by Pioneer 11 satellite in the Dione orbital access channel (6.26 Rs) [5] later [6] also confirmed the existence of similar magnetic oscillations coupled to O^+ ion population between 5 - 7 Rs observed by Voyager 1. The CAPS magnetometer reported the ion cyclotron waves linked with water group ions (O^+, OH^+, H_2O^+ and O_2^+) again on Cassini's orbit insertion throughout the E ring approximately all the local times with maximum peak close to equator [7], frequencies of these wave found to be close to the local water group ion cyclotron frequency. Recently [21] examined the strong evidences of EMIC wave between 5-7 RS and found that the amplitude of the ion cyclotron wave remains almost static in between Enceladus orbits (L = 3.9) and the orbits of Dione (L = 6.3).

Analysis of ion cyclotron wave becomes important as it works as a diagnostic tool in order to prob magnetospheric dynamical processes gives insight into the composition of plasma particles [22]. Galileo measurements of Io pass provided demonstrable understanding in view of temperature anisotropy which believed to be originated due to newly created ions from sulphur dioxide and sulphur monoxide due to impact of solar radiations and high energetic electron in the outer layer of Io [23,24], calculated mass loading with high accuracy. Loss rate of the particles from E ring neutral cloud by [7] and Ion production rate estimated by [25] and [26] using amplitudes of these waves.

The study characterises the growth of ion cyclotron wave with respect to various factors and local conditions based on the literature survey and previous work done in Saturn's inner magnetosphere. The work considers the effect of ion cyclotron wave on pickup ions opting ring distribution with background cold plasma and provide the better estimation for growth rate of EMIC wave by developing mathematical dispersion model by using kinetic approach.

2. Empirical dispersion model

Dispersion relation and Growth rate - An empirical dispersion model is presented here and analysed based on communicated data appraising local plasma conditions, it is evident that planetary magnetosphere is considered to have anisotropic and collision less plasma thus perturb and unperturbed state of charged particle may arrive due to introduced instabilities and wave particle interaction. Method of characteristics is opted here to establish dispersion relation exposing controlling factors for growth rate by considering anisotropic, homogeneous and collision less plasma. The approach gives impeccable estimation for perturb state of particles in terms of any arbitrary distribution function. Method has good scope to get clear idea about Doppler shift as calculation includes sum and difference of alternating field term and covers nonlinear interaction part.

Dispersion Model for growth rate is developed for collision less, anisotropic and homogeneous, taking small inhomogeneity is only presumed in interaction zone. Here considering the same direction of Magnetic field as well as electric field i.e., both in z direction with magnitude $\boldsymbol{B} = \boldsymbol{B_o}\hat{\boldsymbol{e}}_{\boldsymbol{z}}$ and electric field $\boldsymbol{E} = \boldsymbol{E_o}\sin \mathbf{vt}\hat{\mathbf{e}}_{\boldsymbol{z}}$. The mathematical model necessitate lenearization of Vlasov Maxwell equations to avoid other higher terms in order to achieve particle trajectories of perturbed distribution function and dispersion model.

Dispersion modal is derived here for relativistic case in the omnipresence of parallel AC electric field for n=1 keeping the same approach opted by [27]. The numerical outcome of dielectric constant is given here implying vlasov equation by solving other essential parameters as particle trajectories, perturbed distribution function, conductivity tensor.

$$\frac{k^2c^2}{\omega^2}=1+\sum_s\frac{4e_s^2\pi}{\omega^2}\sum_p J_p\left(\lambda_2\right)\int\frac{d^3v}{2}v_\perp\left[\begin{array}{l}\left(\omega-k_\parallel v_\parallel\right)\frac{\partial f_o}{\partial v_\perp}\\ -k_\parallel\frac{\partial f_o}{\partial v_\perp}\frac{\Gamma_{\parallel s}}{\nu}\left(\frac{p}{\lambda_2}-1\right)\\ +k_\parallel v_\perp\frac{\partial f_o}{\partial v_\parallel}\end{array}\right]*\left(\frac{1}{\omega-k_\parallel v_\parallel-\frac{k_\parallel\Gamma_{\parallel s}}{\nu}+p\nu\pm\omega_c}\right)$$

…(1)

Maxwellian ring distribution (Bi Maxwell) function employed here to find unperturbed phase space density of captured electron particle [28].

$$f(v_\perp,v_\parallel)=\frac{n_s/n}{\pi^{3/2}\alpha_{\parallel s}\alpha_{\perp s}^2 A}\exp\left[-\frac{\left(v_\perp-v_o\right)^2}{\alpha_{\perp s}^2}-\frac{\left(v_\parallel^2\right)}{\alpha_{\parallel s}^2}\right]$$

…(2)

$$A=\exp\left(-\frac{v_o^2}{\alpha_{\perp s}^2}\right)+\sqrt{\pi}\left(\frac{v_o}{\alpha_{\perp s}}\right)\operatorname{erfc}\left(-\frac{v_o}{\alpha_{\parallel s}}\right)$$

…(3)

Where s denotes species and in the present case electrons and ions are considered,

$$\alpha_{\parallel e}=\left(2k_bT_{\parallel e}/m_e\right)^{1/2},\ \alpha_{\perp e}=\left(2k_bT_{\perp i}/m_e\right)^{1/2},\ \alpha_{\parallel i}=\left(2k_bT_{\parallel i}/m_i\right)^{1/2}\text{ and }\alpha_{\perp i}=\left(2k_bT_{\perp i}/m_i\right)^{1/2}$$

Here parameters are showing parallel and vertical thermal velocities of particles (ions and electrons). n_s/n in equation (2) represents the ratio of electron-to-electron total density captured and characterized by high energy, whereas complementary error function is denoted by erfc(x).

Here v_o is symbolized as drift velocity and finally perpendicular and parallel thermal velocities are represented as $v_\perp$ and $v_\parallel$.

Attempting the integration for density $d^3v=2\pi\int_0^\infty v_\perp dv_\perp\int_{-\infty}^\infty dv_\parallel$ and using equation 1 and equation 2, finally the expression for dispersion relation is achieved as:

$$\frac{k^2c^2}{\omega^2}=1+\frac{4e_s^2\pi}{\omega^2}\sum_p J_p\left(\lambda_2\right)\frac{\left(n_s/n\right)}{A}\left[\frac{1}{\alpha_{\parallel s}}\left(\frac{\omega}{k_\parallel}-\frac{\Gamma_{\parallel s}}{\nu}\left(\frac{p}{\lambda_2}-1\right)\right)X_1Z\left(\xi\right)+X_2\left(1+\xi Z\left(\xi\right)\right)\right]$$

…(4)

Here Ions are assumed to have anisotropic distribution, hence taking the term $T_{\perp i}>T_{\parallel i}$ and $\left|k_\parallel\alpha_{\parallel i}\right|<<\left|\omega_r\pm\omega_{ci}+i\gamma\right|$ under consideration.

The above dispersion relation is now approximated in ion cyclotron range of frequencies. Therefore, predicating the thermal effect of electrons as $T_{\perp e} = T_{\| e} = T_e$ with $\left|\omega_r + i\gamma\right| << \omega_{ci}$Considering these approximations, equation (4) showing dispersion term is reduced to:

$$D(k,\omega_r + i\gamma) = 1 - \frac{k^2c^2}{\left(\omega_r + i\gamma\right)^2} + \sum_p J_p\left(\lambda_2\right)\left[\begin{array}{l} \left(\frac{\omega_{pe}^2}{\omega_{ci}^2} - \frac{\omega_{pe}^2}{\left(\omega_r + i\gamma\right)\left(\pm\omega_{ci}\right)}\right) X_{1e} \\ + \frac{\omega_{pi}^2}{\left(\omega_r + i\gamma\right)^2}\left(\begin{array}{l} X_{1i}\frac{1}{\alpha_{\|i}}\left(\frac{\omega_r + i\gamma}{k_\|} - \frac{\Gamma_{\|i}}{\beta\nu}\left(\frac{p}{\lambda_2} - 1\right)\right) Z\left(\xi_i\right) \\ + X_{2i}\left(1 + \xi_i Z\left(\xi_i\right)\right) \end{array}\right) \end{array}\right] \quad \ldots(5)$$

where

$X_{1i} = 1 + \frac{v_o^2}{\alpha_{\perp i}^2} - \sqrt{\pi}\frac{v_o}{\alpha_{\perp i}}$,

$X_{1e} = 1 + \frac{v_o^2}{\alpha_{\perp e}^2} - \sqrt{\pi}\frac{v_o}{\alpha_{\perp e}}$ and

$X_{2i} = X_{1i} + \frac{\alpha_{\perp i}^2}{\alpha_{\| i}^2}\left(1 - \sqrt{\pi}\frac{v_o^3}{\alpha_{\perp i}^3} erfc\left(\frac{v_{\perp i}^{'}}{\alpha_{\perp i}}\right) + 3\frac{v_o^2}{\alpha_{\perp i}^2} - \frac{3}{2}\sqrt{\pi}\frac{v_o}{\alpha_{\perp i}}\right)$

After applying charge neutrality condition $\frac{\omega_{pe}^2}{\pm\omega_{ce}^2} = \frac{-\omega_{pi}^2}{\pm\omega_{ci}^2}$and the condition $\left|\frac{k^2c^2}{\omega^2} >> 1 + \frac{\omega_{pe}^2}{\omega_{ce}^2}\right|$, and solving it, equation 5 becomes

$$D\left(k,\omega_r + i\gamma\right) = -\frac{k_\|^2c^2}{\omega_{pi}^2} + \sum_p J_p\left(\lambda_2\right)\left[\begin{array}{l} \frac{\omega}{\pm\omega_{ci}} X_{1e} \\ + X_{1i}\left\{\frac{1}{\alpha_{\|i}}\left(\frac{\omega}{k_\|} - \frac{\Gamma_{\|i}}{\nu}\left(\frac{p}{\lambda_2} - 1\right)\right) Z\left(\xi_i\right) + \frac{X_{2i}}{X_{1i}}\left(1 + \xi_i Z\left(\xi_i\right)\right)\right\} \end{array}\right] \quad \ldots(6)$$

Now the plasma dispersion function is expressed as:

$Z(\xi) = \frac{1}{\sqrt{\pi}}\int_{-\infty}^{\infty}\frac{e^{-t^2}}{t - \xi}dt$, where $\xi = \frac{\omega - k_\|\Gamma_{\|s} \big/ \nu + p\nu \pm \omega_c}{k_\|\alpha_{\|s}}$

$\omega_{ps}^2 = \frac{4\pi e_s^2 n_s / n}{B}$

Then the wave vector $\tilde{k} = \frac{k_\|\alpha_{\|i}}{\omega_{ci}}$ is a dimensionless parameter came out from the above equation.

2.1 Case I: Dispersion model (parallel): Ion cyclotron wave propagating in the same direction as magnetic field direction

$$\frac{\gamma}{\omega_{ci}} = \frac{\frac{\sqrt{\pi}}{\tilde{k}}\left(\frac{X_{2i}}{X_{1i}} - k_4\right)k_3^3 \exp\left[-\left(\frac{k_3^2}{\tilde{k}}\right)^2\right]}{1 + \frac{\tilde{k}^2}{2k_3^2} + \frac{\tilde{k}^2}{k_3}\left(\frac{X_{2i}}{X_{1i}} - k_4\right) + \frac{m_e}{m_i}\frac{X_{1e}}{X_{1i}}k_3^2} \quad \ldots(7)$$

The real part of equation (7) is

$$(\text{Re freq. } X_3 = -\frac{\omega_r}{\omega_c} = X_4 + \frac{\tilde{k}^2}{2\beta_1}\left[\frac{X_{2i}}{X_{1i}}\frac{\beta_1}{\left(1+X_4\right)} - \frac{\left(1+X_4\right)}{X_{1i}}\right] \quad \ldots(8)$$

Where $k_3 = 1 - X_3 + X_4$, $k_4 = \frac{X_3 - X_4}{1 - X_3 + X_4}$ and

$$\beta_1 = \frac{4\pi\mu_o\varepsilon_o k_b T_{\|i}\left(n_i/n\right)}{AB_o^2}$$

$$X_4 = \frac{k_\| \Gamma_{\|i}}{\nu\omega_c} - \frac{p\nu}{\omega_c} \quad \ldots(9)$$

2.2 Case II: Dispersion model (oblique angle): Ion cyclotron wave propagating obliquely to magnetic field direction

$$\frac{\gamma}{\omega_{ci}} = \frac{\frac{\sqrt{\pi}}{\tilde{k}\cos\theta}\left(\frac{X_{2i}}{X_{1i}} - k_4\right)k_3^3 \exp\left[-\left(\frac{k_3^2}{\tilde{k}\cos\theta}\right)^2\right]}{1 + \frac{\left(\tilde{k}\cos\theta\right)^2}{2k_3^2} + \frac{\left(\tilde{k}\cos\theta\right)^2}{k_3}\left(\frac{X_{2i}}{X_{1i}} - k_4\right) + \frac{m_e}{m_i}\frac{X_{1e}}{X_{1i}}k_3^2} \quad \ldots(10)$$

The real part of equation (10) is

$$\text{(Re freq.) } X_3 = -\frac{\omega_r}{\omega_c} = X_4 + \frac{\left(\tilde{k}\cos\theta\right)^2}{2\beta_1}\left[\frac{X_{2i}}{X_{1i}}\frac{\beta_1}{\left(1+X_4\right)} - \frac{\left(1+X_4\right)}{X_{1i}}\right]$$

3. Results and Discussion

3.1 Plasma Parameters and observation:

Analysis is attributed to observations and plasma conditions and limited to inner middle boundary (< 7 Rs). Here are discussing few relevant monitoring data. [29] first reported the global view of Saturn plasma electron environment by analysing observation from voyager 1 and Voyager 2. [30] performed observational study extensively about at radial distances. The range of temarotene anisotropy ((1-3)) due to an anisotropic distribution of pickup O_+ ions reported by [6] specifically in inner magnetosphere(5-7Rs) causing sufficient wave growth with peak amplitude ~2nT near equatorial plane in the course of Voyager 1 observation. Saturn's inner magnetosphere (5-12 Rs) is populated with two different components i.e. hot (>100ev) and cold component (<100ev) [31-33], radial diffusion of these population in inner magnetosphere is very much expected from the interchanged instability influenced by centrifugal forces. Variable magnetic fields strength was found for the observed range of thermal anisotropy (A_T) by [12], evolving range was between 109.33 and 299.10 nT for ICW and for added harmonics it was 157.19 nT - 363.60 nT, magnetic field strength is not restricted to constant value but different for different region. Study carryout the variation in dimensionless wave growth of parallel and obliquely propagating ion cyclotron waves for the particles in ring distribution near 5 Rs restricted to an angle below 5°. Comprehensive analysis of the result has been performed by taking previous published data set based on Cassini and Voyager 1 spacecraft. Measured magnitude of ambient magnetic field B_o=184 nT. The thermal energy ($K_BT_{||e}$) of electrons is 200 eV and of ions ($K_BT_{||i}$) is 1keV. Number density of ions is considered to be $n_o = 5x10^7\ m^{-3}$ and magnitude of AC electric field E_o= 0.01 mV/m has been considered.

3.2 For Parallel Propagation

Analysing here is the growth of EMIC wave associated with water group ions evolved due to rising temperature anisotropy (A_T) in ion profile distribution followed by calculation of particle perturb trajectory in the presence of an alternating electric field being much smaller than the gyro frequency and plasma frequency. Graph representing the variable growth against the wave number with respect to various parameters.

Figure 1, depicts the parallel propagating G.R. (γ/ω_c) representing growth rate of electromagnetic ion cyclotron wave (EMIC) for the different temperature ratio $T_\perp/T_{||}$ Here numerical simulation shows that for the ratio of vertical to parallel temperature i.e. $T_\perp/T_{||}$ equals to 1.25, the peak (0.133) of G.R. (γ/ω_c) appeared at 0.4 $\tilde{k}$, for the greater value of $T_\perp/T_{||}$ equal to 1.5, the peak (0.135) of G.R. (γ/ω_c) achieved at 0.4 $\tilde{k}$ and for the highest considered value of $T_\perp/T_{||}$ equals to 1.75, maxima (0.137) of growth rate (γ/ω_c) becomes 0.38 $\tilde{k}$. Based on the fact that the value of temparature anisotropy ratio = A_T + 1, it is culminated that as the temperature anisotropy increases, the growth rate seems to be extended with a shift towards lower wavenumber side. Similar result explained by [34] near the plasma pause zone of the Earth.

Figure 2, manifesting growth rate against wave number, plotted for different AC frequency. For the highest considered value of alternating frequency υ = 12 Hz, the peak (0.16959) of growth (γ/ω_c) occurred at 0.44 $\tilde{k}$. When the AC frequency reaches 8 Hz, the peak (0.13296) of G.R. appears at 0.4 $\tilde{k}$. For υ = 4 Hz, the maxima (0.088) of G.R. γ/ω_c shifted to 0.32 $\tilde{k}$. Consistent results have been performed for intensified Whistler mode wave in the orthogonal AC field having loss cone as well as Maxwellian distribution functions [35].

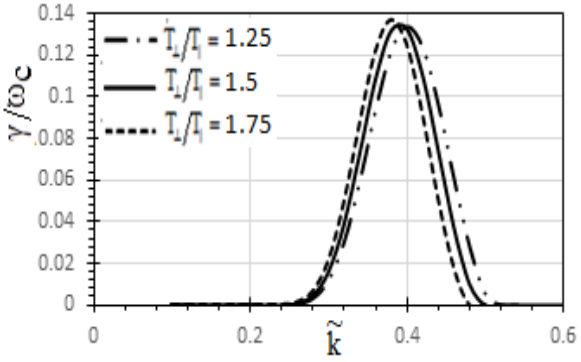

Figure 1. G.R. variant for different $\tilde{k}$ at numerous values of $T_{\perp}/T_{\parallel}$ keeping υ = 8Hz, n_o=5x10^{7}m^{-3} and other plasma parameters constant.

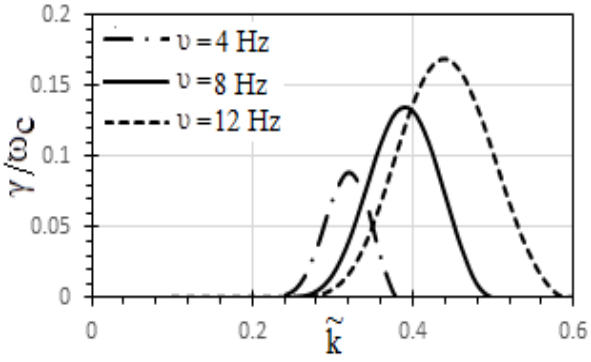

Figure 2. G.R. variant for different $\tilde{k}$ at numerous values of υ keeping $T_{\perp}/T_{\parallel}$ =1.5, n_o=5x10^{7}m^{-3} and other plasma parameters constant.

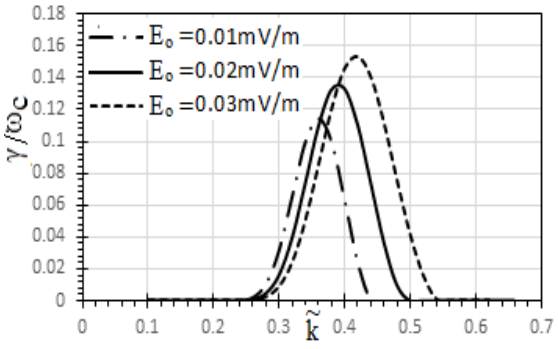

Figure 3. G.R. variant for different $\tilde{k}$ at numerous values of E_o keeping $T_{\perp}/T_{\parallel}$ =1.5, n_o=5x10^{7}m^{-3}, υ = 8Hz and other plasma parameters constant.

In figure 3, growth rate is calculated for numerous values of electric field strength. Consequently, for Eo = 0.01 mV / m, Eo = 0.02 mV / m, Eo = 0.03 mV / m peak of the enhanced wave (γ/ω_c) observed 0.1143, 0.13269, 0.1535 at $\tilde{k}$ = 0.36, 0.4, 0.42 respectively. The corresponding maximum value of $\tilde{k}$ is changed from 0.36 to 0.42. Seemingly, observed wave growth explains that these fluctuating electric field strengths play viable role to produce changes in orthogonal thermal velocity intern changing the vertical component of the energy. Conclusively it is indicative of the enhanced growth of EMIC wave in the presence of such nominal high energy electrons (showing positive slope of the distribution function). Hence can be considered as the prime source of energy for Saturn's magnetosphere.

3.3 For Oblique Propagation

Figure 4, shows the change in growth rate (G.R.) with respect to temperature anisotropy (A_T). From the figure it is visible that the proportion of temperature (perpendicular to parallel) i.e., $T_\perp/T_{||}$= 1.25, maximum G.R. achieved 0.13206 at 0.4 $\widetilde{k}$. When $T_\perp/T_{||}$ becomes 1.5, peak of G.R. (0.1325) is observed again at 0.4 $\widetilde{k}$ and when the ratio referring the value 1.75, G.R. (γ/ω_c) becomes 0.13529 again at 0.4 $\widetilde{k}$. Therefore, the G.R. increases slightly as the equivalent temperature fraction reaches to high value of by enhancing resonance conditions. As the spectrum moves toward the higher wavenumber side, the second harmonic occurs at a higher rate of growth for the higher value of temperature anisotropy. The parallel case discussed earlier does not change much, but temperature anisotropy is believed to support oblique propagation as the highest peak (1.4306) of the maximum growth seems to be appeared at 0.9 $\widetilde{k}$ for the second harmonic along with wider bandwidth spectrum. Therefore, temperature anisotropy remains the primary source of sliding free energy to the plasma. This behaviour of the EMIC wave is similar to the oblique propagation of the Uranus magnetosphere with a parallel alternating electric field [36].

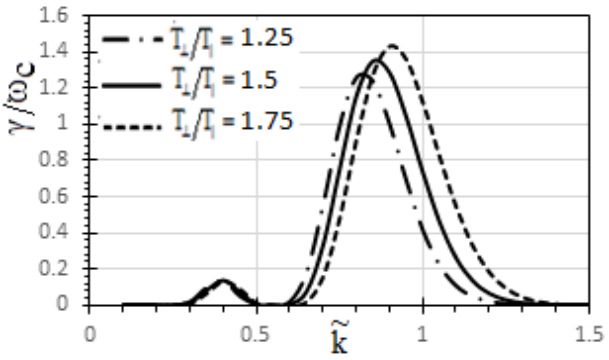

Figure 4. G.R. variant for different $\tilde{k}$ at numerous values of $T_\perp/T_{||}$ keeping θ=2°, n_o=5x10^{7}m^{-3}, υ=8Hz and other plasma parameters constant.

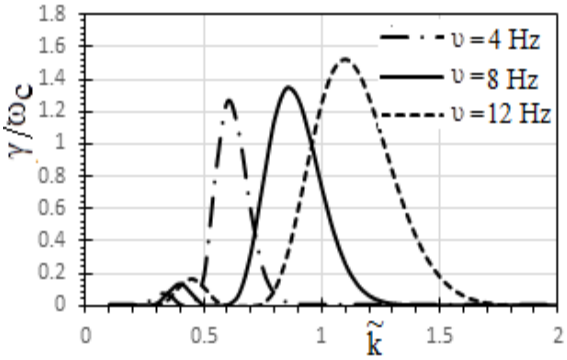

Figure 5. G.R. variant for different $\tilde{k}$ at numerous values of υ keeping θ=2°, n_o=5x10^{7}m^{-3}, $T_\perp/T_{||}$ =1.5 and other plasma parameters constant.

In Figure 5, the curve is a plot of different external AC magnetic field frequency values between growth rate and wavenumber. The peak of the first harmonic is very close to the peak of the parallel propagation. However, for the second harmonic, maximum peak (1.52625) of growth rate γ/ω_coccurs at $\widetilde{k}$ =1.1 for the higher considered value of AC frequency 12 Hz and the maxima of γ/ω_c=1.2624, 1.34976 occurs at $\widetilde{k}$ =0.6 to 0.85 for 4 Hz and 8 Hz respectively. seemly the roll of these frequencies is to enhance the resonance condition and normalization of real frequency (X3 = - ωr/ωci) therefore, as the external frequency increases, the growth rate also increases.

The results are analogous with the work proposed by [37] in the Saturn inner magnetosphere evaluating EMIC wave and [38], proposed analysis on excitation of whistlers propagating obliquely in the Earth's magnetosphere and interplanetary spaces.

Figure 6, shows that the growth rate of the EMIC wave varies with the electric field strength versus the wave number. As can be seen from the figure, as the electric field strength increases, the wave growth increases. For E_o= 0.03 mV/m, maxima (1.5262) of G.R. (γ/ω_c) occurs at 1.1 $\tilde{k}$, showing maximum growth. For E_o= 0.02 mV/m, G. R. (γ/ω_c) maxima (1.425) appears at 1 $\tilde{k}$ and for E_o=0.01 mV/m, G.R. (γ/ω_c) peak 1.34976 in oblique propagation case shifted to 0.85 $\tilde{k}$, Saturn's large rotational axis tilt (sixty degrees) is associated with its magnetic dipole axis introduces unique radio emission conditions.

Figure 7, estimating the effect of the inclined axis on the growth of the Saturn's magnetosphere EMIC wave. Apparently, it is marked that the propagating wave vector is making an angle with magnetic field direction, as the value of the oblique angle between propagating wave and magnetic field increases ($1^o \sim 3^o$), the G.R. increases as well. It is evident from the figure that for the lowest value of angle $1^o\theta$ the peak (0.12876) of the G.R. came at 0.4 $\tilde{k}$, the peak value G.R. shifts to 0.13529 for slightly greater angle $2^o\theta$ occurs at 0.4 $\tilde{k}$ and for $\theta = 3^o$ the peak value (0.1355) of G.R. γ/ω_c repetedly appears at 0.45 $\tilde{k}$. Results may achieve due to variability of density phase space. Seemingly after 5°, the ion cyclotron wave could not be found.

The graph thus drawn also evaluates that the maximum peak of the second harmonic is γ/ω_c=1.34976 (for $\theta = 1^o$) , γ/ω_c=1.4258 (for $\theta = 2^o$) , γ/ω_c =1.4592 (for $\theta = 3^o$) at 0.85 $\tilde{k}$,0.9 $\tilde{k}$, and 1 $\tilde{k}$ respectively. Similar results were found by [39] for electrostatic ion cyclotron waves.

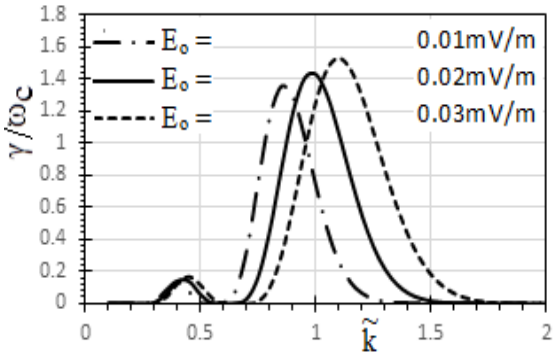

Figure 6. G.R. variant for different $\tilde{k}$ at numerous values of E_o keeping θ=2°, n_o=5x10^{7}m^{-3}, $T_\perp/T_{||}$ = 1.5, υ = 8Hz and other plasma parameters constant.

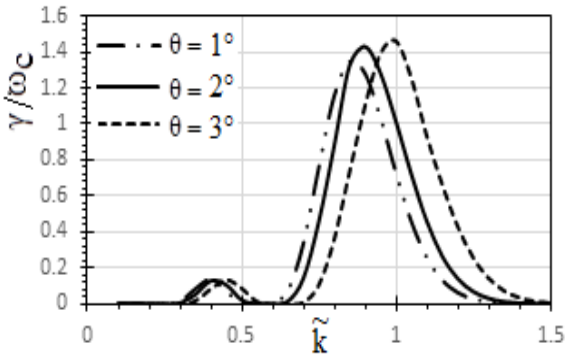

Figure 7. G.R. variant for different $\tilde{k}$ at numerous oblique angles keeping $T_\perp/T_{||}$ =1.5, n_o=5x10^{7}m^{-3}, υ = 8Hz and other plasma parameters constant.

It can be seen from the above evaluation that for the increasing value of A_T bandwidth decreases and growth rate increases. In general, when the maxima shift toward the lower value i.e., $\tilde{k}$ < 0.1.5 is infect a clear indicative of quenched instability showing depleted velocity as compere to thermal speed and showing possibility of low frequency emission for the enhanced Landau damping and considered increase in real frequency term. Variable AC frequency also showing important effects through broad bands indicating VLF emissions.

4. Conclusion

The result demonstrates the analysis of the enhanced EMIC wave in view of E ring captured ions along equatorial plane near 5Rs at lower latitude in Saturn magnetosphere by using the eigen solution method. Computation of evolving growth rate of left-handed EMIC wave and actual frequency has been attempted

for positive ions keeping alternating field in existence by opting kinetic approach. Established linear dispersion model confirms the critical temperature anisotropy in positive ions and involvement of AC frequency causing wave growth. Results are in great agreement with the outcome proposed by Barbosa [6], Rodríguez et al [12] in terms of temperature anisotropy. The introduced alternating frequency found to be one of the most viable parameters in view of enhancing resonance condition minimizing the factor $X3 = -\omega r/\omega ci$ and inferring the growth of ion cyclotron waves. The outcome is analogous with the result proposed by Pandey et al [37]. More assertively comparative study of parallel and oblique propagation of EMIC waves has been done here through a comprehensive mathematical analysis. It is found that the growth of the EMIC wave propagating obliquely with Saturn's intrinsic magnetic field is greater than that of propagating parallel to the direction of the magnetic field. Therefore, in case of Saturn magnetosphere, the higher wavenumber range results in a higher energy range for the medium ion wave. The analysis provides a better outlook of high-energy particles in comparison of Voyager 2 observation in Saturn's magnetosphere. Further the study is applicable in search of the nature of the instability causing Whistler mode wave growth in the outer radiation band of anisotropic high-energy particle components in Saturn or other spatial plasmas. Future work also suggests the study of modified EMIC wave at larger latitudes (may include various radial distance) to examine harmonics of these waves believed to be associated with critical high temperature anisotropy and can be extended to analyse pitch angle scattering mechanism changing plasma characteristics and local loss processes in inner magnetosphere.

References

[1] Richardson J D 1998 Thermal plasma and neutral gas in Saturn's magnetosphere *Rev. Geophys.* **36 4** pp 501–24

[2] Persoon A M, Gurnett D A, Kurth W S, Hospodarsky G B, Groene J B, Canu P and Dougherty M K 2005 Equatorial electron density measurements in Saturn’s inner magnetosphere *Geophys. Res. Lett.* **32** L23105 doi:101029/2005GL024294

[3] Esposito L W et al 2005 Ultraviolet imaging spectroscopy shows an active Saturnian's system *Science* **307** pp 1251-55

[4] Jurac S, McGrath M A, Johnson R E, Richardson J D, Vasyliunas V M and Eviatar A 2002 Saturn: Search for a missing water source *Geophys. Res. Lett.* **29** 24 p 2172

[5] Smith E J and Tsurutani B T 1983 Saturn's magnetosphere: Observations of ion cyclotron waves near the Dione L shell *J. Geophys. Res.* **88** pp 7831-36

[6] Barbosa D D 1993 Theory and observations of electromagnetic ion cyclotron waves in Saturn's inner magnetosphere *J. of Geophys. Res.* **98** pp 9345-50

[7] Leisner J S, Russell C T, Dougherty M K, Blanco-Cano X, Strangeway R J and Bertucci C 2006 Ion cyclotron waves in Saturn’s E ring: Initial Cassini observations *Geophys. Res. Lett.* **33** L11101 doi:101029/2005GL024875

[8] Dougherty M K et al 2004 The Cassini magnetic field investigation: Overview of arrival science *Space Sci. Rev.* **114** pp 331-83

[9] Menietti J D, Averkamp T F and Kurth W S 2019 Survey of Saturn whistler mode hiss intensity *Journal of Geophysical Research: Space Physics* **124** 4266-77 https://doiorg/ 101029/2019JA026656

[10] Guan C Y, Shang X J, Xie Y Q et al 2020 Generation of simultaneous H+ and He+ band EMIC waves in the nightside radiation belt *Sci. China Tech. Sci.* **63** pp 2369-74

[11] Young D T et al 2004 Cassini plasma spectrometer investigation *Space Sci. Rev.* **114** pp 111-2 doi:101007/s11214-004-1406-4

[12] Rodríguez-Martínez M, Blanco-Cano X, Russell C T, Leisner J S, Wilson R J and Dougherty M K 2010 Harmonic growth of ion-cyclotron waves in Saturn's magnetosphere *J. of Geophys. Res.***115** A09207 doi:101029/2009JA015000
[13] Russell C T, Leisner J S, Khurana K K, Dougherty M K, Blanco-Cano X and Fox J L 2005 Ion cyclotron waves in the Saturnian magnetosphere associated with Cassini's engine exhaust *Geophys. Res. Lett.* **32** L14S01
[14] Kivelson M G, Khurana K K, Walker R J, Russell C T, Linker J A, Southwood D J and Polanskey C 1996 Ion's interaction with the plasma torus: Galileo magnetometer report *Science* **274** pp 396–8
[15] Lee M A 1989 Ultra-low frequency waves at comets in Plasma Waves and Instabilities at Comets and in Magnetospheres *Geophys. Monogr. Ser.* **53** pp 13–29
[16] Clark G, Paranicasc C, Santos-Costab D, Livib S, Kruppd N, Mitchellc D G, Roussosd E and Tsengb W L 2014 Evolution of electron pitch angle distributions across Saturn's middle magnetospheric region from MIMI/LEMMS *Planet Space Sci.* **104** pp 18-28
[17] Burch J L J, Goldstein T W, Hill D T, Young F J, Crary A J, Coates N, Andre´ W S, Kurth and E C Sittler Jr 2005 Properties of local plasma injections in Saturn's magnetosphere *Geophys. Res. Lett.* **32** L14S02 doi:101029/2005GL022611
[18] Hill T W, Rymer A M, Burch J L, Crary F J, Young D T, Thomsen M F, Delapp D, Andre N, Coates A J and Lewis G R 2005 Evidence for rotationally driven plasma transport in Saturn's magnetosphere *Geophys. Res. Lett.* **32** L14S10 doi:101029/2005GL022620
[19] Paranicas C, Mitchell D G, Roelof E C, Mauk B H, Krimigis S M, Brandt P C, Kusterer M, Turner F S, Vandegriff J, Krupp N 2007 Energetic electrons injected into Saturn's neutral gas cloud *Geophys. Res. Lett.* **34** L02109 doi: 101029/2006GL028676
[20] Blanco-Cano X 2004 Wave generation in moon-satellite interactions *Adv. Space Res.* **33** 2078-91
[21] Meeks Z, Simon S and Kabanovic S 2016 A comprehensive analysis of ion cyclotron waves in the equatorial magnetosphere of Saturn *Planet Space Sci.* **129** pp 47–60
[22] Russell C T and Blanco-Cano X 2007 Ion-cyclotron wave generation by planetary ion pickup *J. Atmos. Sol. Terr. Phys.* **69** pp 1723-38
[23] Huddleston D E, Strangeway R J, Warnecke J, Russell C T and Kivelson M G 1998 Ion cyclotron waves in the Io torus: Wave dispersion free energy analysis and SO_2^+ source rate estimates *J. of Geophys. Res.* **103** pp 19887-900
[24] Russell C T, Blanco-Cano X and Kivelson M G 2003 Ion cyclotron waves in Io's wake region *Planet Space Sci.* **51** pp 233-8
[25] Cowee M M, Omidi N, Russell C T, Blanco-Cano X and Tokar RL 2009 Determining ion production rates near Saturn's extended neutral cloud from ion cyclotron wave amplitudes *J. of Geophys. Res.* **114** A04219 doi:101029/2008JA013664
[26] Huddleston D E and Johnstone A D 1992 Relationship between wave energy and free energy from pickup ions in the Comet Halley environment *J. of Geophys. Res.* **97** A8 pp 12217-29
[27] Kumari J and Pandey RS 2018 Whistler mode waves for ring distribution with AC electric field in inner magnetosphere of Saturn *Astrophys. Space Sci.* **363** p 249
[28] Wu C S, Yoon P H and Freund H P 1989 A theory of electron cyclotron waves generated along uroral field lines observed by ground facilities *Geophys. Res. Let.* **12** p 1461
[29] Sittler E C Jr, Ogilvie K W and Scudder J D 1983 Survey of low energy plasma electrons in Saturn's magnetosphere: Voyager 1 and 2 J. *Geophys. Res.* **88** pp 8847 -70
[30] Gurnett D A et al 2005 Radio and plasma wave observations at Saturn from Cassini's approach and first orbit *Science* **307** p 1255
[31] Mauk B H et al 2005 Energetic particle injections in Saturn's magnetosphere *Geophys. Res. Lett.* **32** L14S05 doi:101029/2005GL022485

[32] Rymer A M, Mauk B H, Hill TW, Paranicas C, André N, Sittler Jr E C, Mitchell D G, Smith H T, Johnson R E, Coates A J, Young D T, Bolton S J, Thomsen M F and Dougherty M K 2007 Electron sources in Saturn's magnetosphere *J. Geophys. Res.* **112** A02201 doi: 101029/2006JA012017
[33] Young D T et. al, 2005 Composition and dynamics of plasma in Saturn's magnetosphere *Science* **307** p 5713 1262 DOI: 101126/science1106151
[34] Ahirwar G 2012 Study of electromagnetic electron cyclotron waves around plasma-pause region *Res. J. Engineering Sci.* 1 **6** p 18
[35] Pandey R P, Singh K M and Pandey RS 2001 A theoretical study of the whistler mode instability at the Uranian bow shock *Earth Moon and Planets* **87** pp 59-71
[36] Pandey R S, Kumar S and Kumar M 2012 Oblique propagating whistler mode wave with parallel AC electric field at magnetosphere of Uranus *Journal of Theoretical and Applied Physics* **6** p 31
[37] Kumari J, Kaur R and Pandey R S 2018 Effect of hot injections on electromagnetic ion-cyclotron waves in inner magnetosphere of Saturn *Astrophys. Space Sci.* **363** p 33
[38] Pandey R S and Misra K D 2002 Excitation of oblique whistler waves in magnetosphere of Earth and in interplanetary spaces at 1 AU *Earth Planets Space* **54** pp 159-165
[39] Pandey R S, Misra K D and Tripathi A K 2003 Generation of electrostatics Ion-Cyclotron like Wave by Parallel Flow Velocity Shear in the presence of Inhomogeneous Electric Field in an Anisotropic Magneto-plasma *Indian Journal of Radio &Space Physics* pp 3075-82